Scrutinizing the relationship between major physiological and compositional changes during 'Merryl O'Henry' peach growth with brown rot susceptibility

Núria Baró-Montel, Jordi Giné-Bordonaba*, Rosario Torres, Núria Vall-llaura, Neus Teixidó and Josep Usall

Postharvest Department, Institute of Agrifood Research and Technology (IRTA), Edifici Fruitcentre, Parc Científic i Tecnològic Agroalimentari de Lleida, Parc de Gardeny, 25003 Lleida, Catalonia, Spain.

*Corresponding author: Jordi Giné-Bordonaba

Phone: +34973032850 ext. 1597

E-mail: jordi.gine@irta.cat

DECLARATION OF CONFLICTING INTERESTS

The author(s) declared no potential conflicts of interest with respect to the research, authorship, and /or publication of this article.

FUNDING

The authors disclosed receipt of the following financial support for the research, authorship, and/or publication: The Ministry of Economy and Competitiveness (Government of Spain) with the projects AGL2014-55287-C02-02-R and AGL2017-84389-C2-1-R, the Catalan Government (Generalitat de Catalunya) with the PhD grant 2017FI_B1_00153 to Núria Baró-Montel, and the CERCA Programme / Generalitat de Catalunya.

The authors would also like to thank Albert Estévez for their technical assistance.

ORCID ID

N. Baró-Montel 0000-0003-2561-9304

J. Giné-Bordonaba 0000-0001-8514-5337

R. Torres 0000-0002-1806-9626

N. Vall-llaura 0000-0002-7054-7461

N. Teixidó 0000-0002-1676-3592

J. Usall: 0000-0002-0856-3508

47 **Abstract**

48 In the present work, the major physiological and compositional changes occurring during
49 'Merry'l O'Henry' peach growth and its relationship with susceptibility to three strains
50 of *Monilinia* spp. at 49, 77, 126 and 160 d after full bloom (DAFB) were explored. Results
51 of disease incidence indicated wide differences among phenological stages, being 49 and
52 126 DAFB the moment when peaches showed significantly lower susceptibility to brown
53 rot (40% and 23% of rotten fruit, respectively, for strain ML8L). Variation in brown rot
54 susceptibility among different growth stages was also strain-dependent. Lower fruit
55 susceptibility to ML8L at 49 and 126 was accompanied by noticeable changes in the fruit
56 ethylene and respiration patterns, and also in sugars and organics acids content. By
57 employing a Partial Least Squares (PLS) regression model, a strong negative relationship
58 between citric acid, and a positive association of ethylene with peach susceptibility to
59 *Monilinia* spp. at diverse phenological stages was observed. The results obtained herein
60 highlight that the content of certain compounds such as citrate, malate and sucrose, the
61 respiratory activity and the fruit ethylene production may mediate in a coordinated
62 manner the fruit resistance to *Monilinia* spp. at different phenological stages of peach
63 fruit.

64

65 **Keywords:** citric, ethylene, fruit development, *Monilinia* spp., *Prunus persica*.

66

67 **INTRODUCTION**

68 The causal agent of brown rot (*Monilinia* spp.) is able to infect peach fruit at any stage of
69 stone fruit development (Byrde and Willets, 1977) either with the presence of an opening
70 (i.e., stomata, lenticels, wounds, micro-cracks) or through contact with an intact surface

(Rungjindamai et al., 2014). After conidial germination, the fungus produces germ tubes and appressoria, (Garcia-Benitez et al., 2017; Lee and Bostock, 2006) which penetrate the fruit surface yet depending on the environmental conditions (Rungjindamai et al., 2014) as well as the fruit developmental stage.(Oliveira et al., 2016) In this sense, the growth and ripening of fleshy fruit is typically accompanied by numerous biochemical and physiological changes, such as activation of key hormones, including ethylene, and cell-wall loosening enzymes, increase of soluble sugars or decline of acidity, among others, that are somehow synchronised with changes in brown rot susceptibility (De Cal et al., 2013; Garcia-Benitez et al., 2017).

Biochemical approaches in *Monilinia* spp.-stone fruit pathosystem have been used to explain resistance in unripe fruit. Phenolic compounds have been repeatedly linked with higher resistance to *M. fructicola* by its action in inhibiting cutinase activity (Bostock et al., 1999; Lee et al., 2010; Lee and Bostock, 2007; Wang et al., 2002). Similarly, an inhibitory effect of chlorogenic and neochlorogenic acids, compounds that tend to be higher in unripe fruit, (Bostock et al., 1999) had been reported as crucial for *M. laxa* pathogenicity by interfering with fungal melanin biosynthesis (Villarino et al., 2011). Regarding the molecular determinants of the fruit ripening-associated changes in brown rot susceptibility, scarce information is relatively available (Baró-Montel et al., 2019). Guidarelli et al. (2014) compared the gene expression profile between susceptible (two weeks before the pit hardening) and resistant (pit hardening) peach fruit developmental stages, finding noteworthy changes in phenylpropanoid and jasmonate-related genes. In addition, a recent study have pointed out the differential role that ethylene plays in the interaction *Monilinia* spp.-stone fruit (Baró-Montel et al., 2019). Accordingly, ethylene might have an effect not only on inducing defence responses to both abiotic and biotic stress in the plant, but on promoting susceptibility to certain fruit pathogens (Chagué et

al., 2006; Shigenaga and Argueso, 2016). From the studies listed above it is clear the complexity and sometimes controversial results obtained for fruit-pathogen interaction studies and especially when considering different phenological stages.

In particular, for brown rot, relatively little information exists explaining what specific changes on the host may account for the observed differences along different phenological stages. Accordingly, this study was performed to further explore changes along development and ripening of peaches (host) and their potential relationship with brown rot (pathogen) susceptibility. To this aim, peaches were characterised at a morphological, physiological and biochemical level at potential moments for infection, and inoculated with *M. fructicola* and *M. laxa*, the main causal agents of brown rot in Europe. Finally, all these data were integrated into a chemometric approach in order to understand the relationship among all the investigated variables.

MATERIAL AND METHODS

Plant material and experimental design

Experiments were conducted with 'Merryl O'Henry' peaches (*Prunus persica* (L.) Batch) obtained from an organic orchard located in Vilanova de Segrià (Lleida, Catalonia, NE Spain). Fruit that were free of physical injuries and rot were picked at successive developmental stages. The growth stages were based on d after full bloom (DAFB), being full bloom the stage when at least 50% of flowers were open, and framed in the BBCH scale (Meier et al., 1994) as follows: 20 (BBCH = 71), 49 (BBCH = 72), 77 (BBCH = 76), 112 (BBCH = 77), 126 (BBCH = 81) and 160 (BBCH = 87) DAFB.

After each harvest, peaches were immediately transported to IRTA facilities under acclimatised conditions (20 °C). Upon arrival at the laboratory, fruit were separated into three different batches depending on whether they were used for: i) morphological and

physiological analysis, ii) biochemical analysis, and iii) assessment of brown rot susceptibility. Morphological and physiological analysis were conducted with 4 replicates of 5 fruit each, 20 fruit per each phenological growth stage; biochemical analysis was conducted with 3 replicates of 5 fruit each, 15 fruit per each phenological growth stage, and assessment of brown rot susceptibility was conducted with 4 replicates of 10 fruit each, thereby assessing 40 fruit per each phenological growth stage and strain inoculated. For biochemical measurements, samples of peel and pulp tissue (10 mm diameter and 5 mm deep) were collected using a cork borer and immediately frozen with liquid nitrogen. Afterwards, samples were lyophilised in a freeze-dryer (Cryodos, Telstar S.A., Terrassa, Spain) operating at 1 Pa and -50 °C for 5 d and grounded prior to being kept at -80 °C until further biochemical analysis. At 20 and 112 DAFB only morphological and physiological analysis were carried out.

Morphological and physiological changes during fruit development and ripening

Fruit growth rate

Fruit weight was measured by using a digital balance and expressed in g, whereas fruit diameter was determined at the equatorial section of the fruit with an electronic digital calliper (Powerfix, Ilford, UK) and expressed in millimetres (mm).

Fruit ethylene production and respiration rate

Ethylene production and fruit respiration were determined as described elsewhere (Baró-Montel et al., 2019). Four replicates of 5 fruit each were placed in sealed flasks of different volumes, in an acclimatised chamber at 20 °C, equipped with a silicon septum for sampling the gas of the headspace after 2 h incubation.

Biochemical changes during fruit development and ripening

143 **Determination of pH**

144 Freeze-dried powder of each sample was rehydrated in purified water obtained using
145 Elix® Advantage water purification system E-POD (Merck KGaA, Darmstadt, Germany)
146 and homogenised using an Ultra-Turrax (IKA Ultra-Turrax® T25 Digital, IKA®-Werke
147 GmbH & Co. KG, Munich, Germany). The amount of water added to each sample was
148 calculated based on the weight loss after freeze-drying. Subsequently, the pH was
149 measured using a pH meter (Model GLP22, Crison Instruments S.A., Barcelona, Spain)
150 with a penetration electrode (5231 Crison).

151 **Determination of fructose, glucose and sucrose content**

152 Soluble sugars were extracted from freeze-dried powder of each sample as described by
153 Giné-Bordonaba et al. (2017) with some modifications. Fifty mg of each sample were
154 diluted in 1 mL of 62.5% (*v/v*) aqueous methanol solvent and placed in a thermostatic
155 bath at 55 °C for 15 min, mixing the solution with a vortex every 5 min to prevent
156 layering. Then, the samples were centrifuged at 24,000 × *g* for 15 min at 20 °C.

157 The supernatants of each sample were recovered and used for enzyme-coupled
158 spectrophotometric determination of glucose and fructose (hexokinase / phosphoglucose
159 isomerase) and sucrose (β-fructosidase) using a commercial kit (BioSystems S.A.,
160 Barcelona, Spain) and following the manufacturer's instructions. Results were expressed
161 on a standard fresh weight basis (g kg^{-1}) and on fruit basis (g per fruit). The
162 monosaccharides / disaccharides (M/D) ratio was determined as the amount of fructose
163 and glucose divided by the amount of sucrose.

164 **Determination of malic, citric and gluconic acids content**

165 Organic acids were extracted from freeze-dried powder of each sample as described by
166 Giné-Bordonaba et al. (2017) with some modifications. Fifty mg of each sample were

diluted in 1 mL of distilled water and placed at room temperature for 10 min, mixing the solution with a vortex every 5 min to prevent layering. Then, the samples were centrifuged at 24,000 × *g* for 5 min at 20 °C.

The supernatants of each sample were recovered and used for enzyme-coupled spectrophotometric determination of malic (L-malate dehydrogenase), citric (citrate lyase / malate dehydrogenase) and gluconic (gluconate kinase / 6-phosphogluconate dehydrogenase) acids, using commercial kits (BioSystems S.A., Barcelona, Spain) and following the manufacturer's instructions. Results were expressed on a standard fresh weight basis (g kg^{-1}) and on fruit basis (g per fruit).

Determination of malondialdehyde

Malondialdehyde (MDA) was analysed as an index of lipid peroxidation using the thiobarbituric acid reactive substrates (TBARS) (Giné-Bordonaba et al., 2017). Five hundred mg of each sample were homogenized in 4 mL of 0.1% trichloroacetic acid (TCA) solution. Then, the samples were centrifuged at 23,300 × *g* for 20 min at 20 °C and 0.5 mL of the supernatant was added to 1.5 mL of a 0.5% thiobarbituric acid (TBA) in 20% TCA solution. Another aliquot (0.5 mL) of the supernatant was added to a solution containing only 20% TCA as a control. The mixture was incubated at 90 °C for 30 min until stopped by placing the reaction tubes in an ice-water bath. Then, the samples were centrifuged at 23,300 × *g* for 10 min at 4 °C, and the absorbance of the supernatant was measured at 532 nm and subtracted to the unspecific absorption read at 600 nm. The amount of MDA-TBA complex (red pigment) was calculated using its molar extinction coefficient 155 mM^{-1} cm^{-1}. Results were expressed on a standard fresh weight basis (µmol kg^{-1}) and on fruit basis (µmol per fruit).

Determination of fruit antioxidant capacity and total phenolic content

191 Extracts for antioxidant capacity (AC) and total phenolic content (TPC) were prepared as
192 described elsewhere (Giné-Bordonaba et al., 2017) with some modifications. Fifty mg of
193 freeze-dried powder of each sample were diluted in 1 mL of 79.5% (*v/v*) methanol and
194 0.5% (*v/v*) HCl aqueous solvent. The mixture was held in the dark at room temperature
195 with constant agitation for 2 h, mixing the solution with a vortex every 15 min to prevent
196 layering. Then, the samples were centrifuged at 24,000 × *g* for 5 min at 20 °C. The
197 supernatants of each sample were recovered and used for spectrophotometric
198 determination.

199 TPC was determined at 765 nm after the reaction of 0.05 mL of each sample extract with
200 0.25 mL of Folin-Ciocalteau reagent, 4.2 mL of Milli-Q water and 0.5 mL of 20% (*p/v*)
201 of Na_2CO_3. Results were expressed on a standard fresh weight basis (g kg^{-1} gallic acid
202 equivalents (GAE)) and on fruit basis (g GAE per fruit). AC was determined at 593 nm of
203 the above mentioned extracts following the Ferric Reducing Antioxidant Power (FRAP)
204 protocol as described by **Giné-Bordonaba and Terry (2016)**. Results were expressed on
205 a standard fresh weight basis (g kg^{-1} Fe^{3+}) and on fruit basis (g Fe^{3+} per fruit).

206 **Determination of ascorbic and dehydroascorbic acids**

207 Extracts for ascorbic (AsA) and dehydroascorbic (dhAsA) acids determination were
208 obtained from 300 mg of freeze-dried powder of each sample that were diluted in 4 mL
209 of 3% (*v/v*) meta-phosphoric acid (MPA) and 8% (*v/v*) acetic acid aqueous solvent. The
210 mixture was homogenised with a vortex for 1 min. Then, the samples were centrifuged at
211 43,000 × *g* for 22 min at 4 °C. The supernatants of each sample were filtered through a
212 0.45 µm filter for High Performance Liquid Chromatography (HPLC) (Millipore,
213 Bedford, MA, USA) and used for HPLC-UV determination protocol as described by
214 Collazo et al. (2018). Results were expressed on a standard fresh weight basis (mg kg^{-1})
215 and on fruit basis (mg per fruit).

Changes in susceptibility to brown rot during fruit development and ripening

In this study three single-spore strains of *Monilinia* spp. were used: *M. fructicola* (CPMC6) and *M. laxa* (CPML11 and ML8L). The strains CPMC6 and ML8L are deposited in the Spanish Culture Type Collection (CECT 21105 and CECT 21100, respectively). All strains were maintained in 20% glycerol (*w/v*) at -80 °C for long-term storage and subcultured periodically on Petri dishes containing potato dextrose agar (PDA; Biokar Diagnostics, 39 g L^{-1}) supplemented with 25% of tomato pulp and incubated under 12-h photoperiod at 25 °C / 18 °C for 7 d.

Conidial suspensions at a concentration of 10^5 conidia mL^{-1} were prepared, and 'Merryl O'Henry' peaches were infected at 49, 77, 126 and 160 DAFB following the methodology described by Baró-Montel et al (2019). All the fruit were incubated in a chamber for a maximum of 14 d at 20 °C and inspected daily to know when disease symptoms initiated. After 7 and 14 d of storage, the number of brown rot infected fruit was recorded.

Statistical analysis

Data were collated and statistically analysed with JMP® software version 13.1.0 (SAS Institute Inc., Cary, NC, USA). Means were compared by analysis of variance (ANOVA) of data expressed on a standard fresh weight basis and on fruit basis, aiming to understand the net assimilation of the target compounds without considering the increase in fruit volume occurring during fruit growth. Values per fruit were calculated using the average value on a standard fresh weight basis multiplied by the average fruit weight (kg) (obtained after weighing 20 individual fruit per each phenological stage). When the analysis was statistically significant, the Tukey's test at the level $p < 0.05$ was performed for separation of means. Significance of correlations between traits was checked by Spearman's rank correlation.

240 A Partial Least Squares (PLS) analysis was conducted, using the same software described
241 above, to find the underlying physiological and biochemical traits (*X* factors) that account for
242 most of the variation in brown rot susceptibility (*Y* response) considering different
243 phenological growth stages. The corresponding data matrix included 12 samples (the
244 triplicate values of each sample at 49, 77, 126 and 160 DAFB) and 19 variables (ethylene,
245 respiration, RQ (respiratory quotient), DW/FW ratio, glucose, fructose, sucrose, M/D
246 ratio, malic acid, citric acid, total gluconic acid, AsA, dhAsA, total AsA (T-AsA), AC,
247 TPC, MDA, pH and incidence for ML8L strain). As a pre-treatment, data for chemometric
248 analysis was centred and autoscaled to provide similar weights for all the variables. The
249 Nonlinear Iterative Partial Least Squares (NIPALS) algorithm with 2 factors was used to
250 estimate the model parameters.

251 **RESULTS**

252 **Morphological changes during 'Merryl O'Henry' development and ripening**

253 The weight and diameter of growing 'Merryl O'Henry' peach fruit were monitored from
254 0 to 160 DAFB (Figure 1(a)). Both parameters followed a double-sigmoid growth curve
255 that hinted three growth phases: i) cell division, ii) pit hardening, and iii) final swell. The
256 first growth phase lasted approximately 50 DAFB with an average growth rate of 0.07 g
257 (R^2 = 0.96) and 0.58 mm (R^2 = 0.99) per d, until fruit reached 4.5 g for weight, and a
258 maximum diameter of 28.6 mm. The phase from 50 to 77 DAFB, registered an average
259 growth rate of 0.96 g (R^2 = 0.97) and 0.29 mm (R^2 = 0.99) per d, until fruit reached a
260 weight of 31 g, and 36.6 mm diameter. This second phase included the hardening period
261 and was characterised by little morphological changes. Finally, the third phase was the
262 period of rapid fruit growth rate with values of 2.7 g (R^2 = 0.99) and 0.52 mm (R^2 = 0.93)
263 of weight and diameter per d, respectively, being greater than those of the earlier phases.
264 In general, there was a strong positive exponential correlation between fruit weight and

diameter (Figure 1(b)). During all the phases, morphological changes in fruit appearances occurred, but most significantly during the latter phase, where the massive fruit growth was accompanied by colour changes (from greenish to yellow and red; Figure 1(c)).

INSERT FIGURE 1

Fruit ethylene production and respiration rate changes during 'Merryl O'Henry' development and ripening

Significant differences in the kinetics of ethylene production were found between 160 DAFB and the earlier sampling points (Figure 2). At the start of the trial, ethylene production was 8 pmol kg^{-1} s^{-1} (Figure 2(a)). Later, it decreased by half, and remained almost undetectable through the second and early third phase. Finally, at 160 DAFB, ethylene production was 15.5 pmol kg^{-1} s^{-1}, coinciding with the climacteric rise. The pattern of net ethylene production per fruit followed the same trend, except for the first 49 DAFB when values were almost zero (Figure 2(b)).

INSERT FIGURE 2

As shown in Figure 2(c), the behaviour on a standard weight basis showed a tendency towards lower amounts of CO_2 released, being the maximum at 0 DAFB (2,718 nmol kg^{-1} s^{-1} CO_2) and the minimum at 122 DAFB (205 nmol kg^{-1} s^{-1} CO_2). The pattern of net CO_2 released (Figure 2(d)), however, was completely opposed, and this was likely cause by the fact that fruit increases in size during development. The net respiratory activity increased constantly throughout fruit development up to 55 nmol s^{-1} CO_2 per fruit at 160 DAFB, coinciding with the ethylene peak. It is noteworthy to mention that a first and transient respiratory peak (32 nmol s^{-1} CO_2 per fruit) was observed at 112 DAFB coinciding also with a peak on the ethylene production on a fruit basis ($R^2 = 0.92$; $p < 0.0001$; Supplemental Figure S1). Regarding RQ, values throughout development were

between 0.73 (49 DAFB) and 1.29 (20 DAFB), fitting the range from 0.7 to 1.3 for aerobic respiration reported for fresh fruit and vegetables (Kader and Saltveit, 2003).

Changes in sugar and acid content during 'Merryl O'Henry' development and ripening

During the course of the experiment, sucrose increased from 7.3 up to 18 g kg^{-1}, being at 160 DAFB significantly higher ($p = 0.0006$) than in earlier sampling points (Figure 3(a)). Overall, fructose showed higher levels than glucose throughout the experiment, with the exception of 49 DAFB. Net accumulation of sucrose, glucose and fructose on a peach basis was evident (Figure 3(b)), and especially during the last month before harvest, when fruit reached their maximum sugar content (4.7, 2.9 and 3.4 g per fruit, respectively). A strong negative correlation was observed between glucose and sucrose ($R^2 = 0.83$; $p = 0.0008$; Supplemental Figure S1), and between fructose and sucrose ($R^2 = 0.69$; $p = 0.0126$; Supplemental Figure S1). Malic acid content ranged from 2 to 9.3 g kg^{-1}, displaying two statistically significant ($p < 0.0001$) peaks at 49 and 160 DAFB (Figure 3(c)). Similar to that observed for sugars accumulation on a fruit basis, malic and citric acid content increased during the course of the experiment, reaching final values of 2.4 and 0.98 g per fruit, respectively (Figure 3(d)). Regarding total gluconic acid, initial values were 0.5 g kg^{-1} (Figure 3(c)). Afterwards, levels for this compound increased by 2-fold, and then decreased progressively until almost zero at 160 DAFB. Unlike other organic acids, total gluconic content on a fruit basis did not display an increase throughout development and ripening. Moreover, the accumulation pattern was the same than on a concentration basis, reaching a maximum of 31 mg per fruit at 77 DAFB and a minimum at harvest.

INSERT FIGURE 3

Changes in antioxidants and malondialdehyde content during 'Merryl O'Henry' development and ripening

Concerning the fruit AC, a transient peak up to 10.72 g kg^{-1} at 77 DAFB was observed (Figure 4(a)). After peaking, AC content decreased until a minimum of 4.89 g kg^{-1} at 160 DAFB. The TPC varied from 1.83 to 4.47 g kg^{-1}, following a pattern similar to that observed for AC, but on a much smaller scale. The results presented on a fruit basis shown a parallel gradual increase of AC and TPC during development (Figure 4(b)), with a significantly higher ($p < 0.005$) amount per fruit at harvest if compared to earlier developmental stages. Our results also evidenced that fruit development was accompanied by an increased accumulation of ascorbate both at a concentration and on a fruit basis, ranging from 1.2 to 78 mg kg^{-1} (Figure 4(c)) and from 0.05 to 21 g per fruit (Figure 4(d)), respectively. In contrast, dehydroascorbate concentration was greatly reduced during fruit growth, reaching a minimum of 17 mg kg^{-1} at 160 DAFB.

In our study, when analysed on a concentration basis (Figure 4(e)), no statistically significant differences in MDA content were observed among the different phenological growth stages. Nevertheless, when analysed on a fruit basis, changes in MDA showed four clearly significant ($p < 0.0001$) levels (Figure 4(f)). MDA content steadily increased throughout fruit growth, and especially during the last month before harvest, where the accumulated levels were over 3-fold than those monitored in earlier phenological growth stages.

INSERT FIGURE 4

Changes in susceptibility to brown rot during 'Merryl O'Henry' development and ripening

337 In addition to the observed physiological and biochemical changes during growth,
338 'Merryl O'Henry' peach fruit also displayed variation in brown rot susceptibility along
339 the different phenological stages (Figure 5). For strains CPMC6 and CPML11, no
340 significant differences were found among the different phenological growth stages.
341 Regarding *M. fructicola*, 100% of the fruit developed the disease. Meanwhile, brown rot
342 incidence for strain CPML11 of *M. laxa* ranged from 90 to 100%. On the contrary, strain
343 ML8L of *M. laxa* showed a wide range of values. Non-wounded peaches artificially
344 inoculated with this later strain showed significantly lesser degree of susceptibility to brown
345 rot at 49 DAFB (40%; $p = 0.0003$) and 126 DAFB (23%; $p < 0.0001$) DAFB. Within these
346 two sampling points (at 77 DAFB), susceptibility significantly increased ($p < 0.0001$) up to
347 75%. Again, increased susceptibility to *Monilinia* infection occurred at 160 DAFB. Taken
348 together, results for ML8L confirmed that susceptibility varied during fruit development,
349 evidencing the sharp increase in susceptibility between 126 DAFB (before the colour
350 break) and 160 DAFB (when epidermis had acquired a uniformly yellow and red colour).

351 INSERT FIGURE 5

352 **Involvement of physiological and biochemical traits in determining changes in**
353 **susceptibility to brown rot**

354 All the data presented herein were integrated on a multivariate analysis to further explore
355 the relationship between the major physiological and biochemical changes occurring
356 during growth with changes in brown rot susceptibility. Although the three strains were
357 able to directly infect non-wounded 'Merryl O'Henry' peaches, the present section focuses
358 on strain ML8L of *M. laxa* since this strain was responsible for the greatest variability in
359 disease incidence among phenological stages. The corresponding loadings plot using the
360 first two PLS factors, accounted for more than 93% of the variation observed (Figure 6).
361 Besides, the correlation between predicted and measured values was high ($R^2 = 0.94$) and

362 led to a highly effective model for predicting ML8L incidence (data not shown). The
363 Variable Importance Plot (VIP) showed that all predictors, except TPC and MDA had
364 values exceeding 0.8 (Figure 6, insert). Cut-off values for the VIP vary throughout the
365 literature, but there is some agreement that values greater than 1.0 indicate predictors that
366 are important (Wold, 1995) within the model. Based on this criterion, DW/FW (1.43),
367 citric acid (1.34), ethylene (1.21), RQ (1.10), malic acid (1.08) and sucrose (1.00) were
368 the most influential variables in determining the PLS projection model and explaining the
369 variable ML8L susceptibility over peach growth in terms of physiological and
370 compositional changes.

371 INSERT FIGURE 6

372 **DISCUSSION**

373 The physiological and biochemical changes that fruit experience throughout development
374 and ripening modify their texture and flavour, leading to fruit suitable for consumption.
375 However, these changes can also cause the fungi to go from a quiescent to a pathogenic
376 state, leading to noticeable changes in fruit susceptibility (Cantu et al., 2008). In this
377 context, phenolic compounds are accounted as a first line of defence against pathogen
378 attack (Yang et al., 2010), and together with phytoalexins and other secondary
379 metabolites, tend to accumulate in regions near the infection as part of a locally induced
380 defences response (Lattanzio et al., 2006). Previous studies (Bostock et al., 1999; Lee and
381 Bostock, 2006) suggest that development of *M. fructicola* in unripe peach fruit was
382 inhibited by phenolic acids. A similar conclusion was drawn for *M. laxa* (Villarino et al.,
383 2011). By comparing different phenological stages, the results from our study do not
384 strictly support these findings since both AC and the TPC were higher in immature
385 'Merryl O'Henry' peach fruit, especially at 77 DAFB (Figure 4), when fruit susceptibility
386 to *Monilinia spp*. was also very high (Figure 5). In this sense, specific compounds rather

than the TPC or AC, or the combination of high antioxidant content with high or low content of other biochemical compounds, are likely involved in the higher resistance to *Monilinia spp*. reported by others (Lee and Bostock, 2006). In our study, special attention was given to ascorbate, a powerful antioxidant and cellular reductant for plants involved in numerous plant responses to biotic stress. Indeed, AsA may act together with glutathione (GSH) and other enzymatic antioxidants via the AsA-GSH cycle providing the correct redox environment to regulate multiple defence pathways including the expression of plant defense genes through the activation of the regulatory transcription factor NPR1 (Nonexpressor of Pathogenesis-Related protein 1), but also modulating hormonal signalling networks involved in plant defense (Boubraki, 2017). Overall, the detected ASA levels in our study were within the range of that found in the literature (30-32) yet no clear associations were found between AsA levels and the fruit susceptibility to *Monilinia spp*.

The sugar content and the ratio between monosaccharides and disaccharides were one of the parameters that mostly varied throughout the development and ripening of 'Merryl O'Henry' peach fruit. Sucrose, glucose and fructose in proportion of about 3:1:1 are the main sugars in peaches (Génard et al., 2003), representing about 75% of total soluble sugars (Crisosto and Valero, 2008). Immature fruit contain starch grains that are rapidly converted into soluble sugars as the fruit mature and ripen (Crisosto and Valero, 2008), and more rapidly during the last few days of maturation on-tree (Ramina et al., 2008). The results regarding sugar changes during growth were in agreement with the literature (Famiani et al., 2016). Sucrose accumulation, occurred mainly during the second exponential growth phase, and may be explained by the up-regulation of genes for hexose transport, together with a gene encoding for sucrose phosphate synthase as reported by others in peach fruit (Nonis et al., 2007). Furthermore, the sharp increase in sucrose levels observed both at a concentration

412 and on fruit basis, was coincident with the ethylene burst. These results, jointly with the
413 strong positive correlation observed between sucrose and ethylene ($R^2 = 0.92$; $p < 0.0001$;
414 Supplemental Figure S1), and between sucrose and respiration ($R^2 = 0.97$; $p < 0.0001$;
415 Supplemental Figure S1), pointed out the key role of this molecule on peach ripening as
416 also observed in other species (Lindo-García et al., 2019). In contrast, glucose and
417 fructose content at harvest reached their minimum (11 and 12.8 g kg^{-1}, respectively),
418 which likely highlights their function as primary photoassimilates for the synthesis of
419 translocated compounds (Osorio and Fernie, 2013) as well as their potential usage as
420 respiratory substrates. Sugars, however, in addition to being the core of primary plant
421 metabolism, have also been implicated in responses to different types of biotic and abiotic
422 stress (Kou et al., 2018). Sugars can be oxidized and induce the production of organic
423 acids (Prusky and Wilson, 2018), as well as a wide range of secondary metabolites which
424 are related to host defence responses (Berger et al., 2007). In the present study, the results
425 of the multivariate analysis revealed that sucrose was positively related to the
426 development of brown rot, pointing out that the catabolism of sucrose could be one of the
427 main sources of carbon and energy that the fungus may use during host colonization. In
428 fact, in *M. fructicola* it has been shown that the progression of the disease is accompanied
429 by a decrease in the content of sucrose and an increase in the content of reducing sugars
430 and soluble solids, as result of the decomposition of this disaccharide into more accessible
431 molecules to the fungus (Kou et al., 2018). Besides, previous studies have already shown
432 that sucrose metabolism and especially invertases play a key role in plant defences against
433 biotic stresses (Tauzin and Giardina, 2014).

434 Like sugars, organic acids are generally considered as important respiratory substrates
435 (Famiani et al., 2016). Our results showed that in 'Merryl O'Henry' peach fruit, organic
436 acids content was highly variable and greatly influenced by the phenological growth

437 stage. Interestingly, the regression coefficients obtained in the present study showed that
438 citric acid was the parameter most negatively correlated with ML8L incidence. A fall in
439 citrate levels of healthy fruit at specific times during growth may lead to greater
440 susceptibility to brown rot which, in turn, may be explained by the loosening of acidity
441 and the antimicrobial activity elicited by this compound (Shokri, 2011). If citrate levels
442 are low within the fruit tissue, the buffering capacity of the fruit is also low and hence it
443 is likely that alkalinisation and acidification, via the secretion of ammonia or organic
444 acids (Prusky et al., 2016) may be easier for the pathogen. In this way, peaches and
445 nectarines infected by *M. fructicola* also showed significant decreases in pH due to the
446 organic acids produced by the fungus (De Cal et al., 2013), supporting the potential role
447 of organic acids in modulating the host environment, as well as enhancing pathogen
448 virulence. In our study, since we are working with healthy peaches neither accumulation
449 of gluconic acid nor changes in pH among the different growth stages were detected.

450 Finally, it is noteworthy to mention that ethylene displayed positive regression
451 coefficients with disease incidence. Ethylene induces fruit ripening as well as plant
452 senescence and many other developmental processes that may be linked to an increased
453 susceptibility to fungal pathogens (Mengiste et al., 2010). During growth, fruit are
454 continuous exposed to various forms of biotic stresses, such as pathogen attack, and
455 ethylene, together with ROS-mediated responses, plays a pivotal role in the activation of
456 signalling pathways related with host defence response to necrotrophic pathogens
457 (Hammond-Kosack and Jones, 1996). The role of ethylene, however, is two-sided since
458 this hormone can promote susceptibility or resistance, depending on multiple factors
459 (Baró-Montel et al., 2019). As a whole, our findings support the crucial role of ethylene
460 in pathogenicity and consequently, let us to hypothesise that the high levels of ethylene
461 jointly with the low and high levels of citric acid and sucrose, respectively, in healthy

462 fruit at 160 DAFB may explain the rise in susceptibility. Concomitantly, the enhanced
463 ethylene production may trigger polygalacturonase (PG) and pectin methyl esterase
464 (PME) (Pech et al., 2008; Wang et al., 2017), especially the former, hence probably
465 facilitating the penetration of the fungus in the fruit tissue.

466 **CONCLUSIONS**

467 The results obtained herein provide a global view of the most relevant changes at
468 morphological, physiological and biochemical level occurring during development and
469 ripening of 'Merryl O'Henry' peach fruit and its relationship to brown rot susceptibility.
470 It is unlikely that specific compounds can account for the lower or higher susceptibility
471 to *Monilinia spp*. along different phenological stages. This said, the content of certain
472 compounds such as citrate, malate and sucrose, the respiratory activity and the fruit
473 ethylene production may co-ordinately act as natural fruit resistance mechanisms to
474 *Monilinia* spp. at diverse phenological stages. A better understanding of these
475 mechanisms may provide a framework for developing more rational control alternatives
476 to synthetic fungicides, and especially for organic production which has been expanding
477 rapidly in most developed countries. In addition, the results from this study also highlight
478 the differential ability of the three strains of *Monilinia* spp. to infect non-wounded
479 peaches. Hence, not only the specie, but each strain-specific mechanisms may have a
480 specific way to colonise the host.

481

482 **REFERENCES**

483 Baró-Montel N, Vall-llaura N, Giné-Bordonaba J, Usall J, Serrano-Prieto S, Teixidó N
484 and Torres R (2019) Double-sided battle: The role of ethylene during Monilinia
485 spp. infection in peach at different phenological stages. *Plant Physiology and*

Biochemistry 144: 324–333. DOI: 10.1016/j.plaphy.2019.09.048.

Berger S, Sinha AK and Roitsch T (2007) Plant physiology meets phytopathology: plant primary metabolism and plant-pathogen interactions. *Journal of Experimental Botany* 58: 4019–4026. DOI: 10.1093/jxb/erm298.

Bostock RM, Wilcox SM, Wang G and Adaskaveg JE (1999) Suppression of *Monilinia fructicola* cutinase production by peach fruit surface phenolic acids. *Physiological and Molecular Plant Pathology* 54(1–2): 37–50. DOI: 10.1006/pmpp.1998.0189.

Boubakri H (2017) The role of ascorbic acid in plant-pathogen interactions. In: Hossain MA, Munné-Bosch S, Burritt DJ, Diaz-Vivancos P, Fujita M and Lorence A (Eds.) *Ascorbic Acid in Plant Growth, Development and Stress Tolerance*. Springer Nature.

Byrde RJW and Willets HJ (1977) *The Brown Rot Fungi of Fruit: Their Biology and Control*. *The Brown Rot Fungi of Fruit*. Oxford: Pergamon Press Ltd. Available at: http://www.sciencedirect.com/science/article/pii/B9780080197401500083.

Cantu D, Vicente AR, Greve LC, Dewey FM, Bennett AB, Labavitch JM and Powell ALT (2008) The intersection between cell wall disassembly , ripening , and fruit susceptibility to *Botrytis cinerea*. 105: 859–864.

Chagué V, Danit L-V, Siewers V, Schulze-Gronover C, Tudzynski P, Tudzynski B and Sharon A (2006) Ethylene sensing and gene activation in *Botrytis cinerea*: a missing link in ethylene regulation of fungus-plant interactions? *Molecular Plant-Microbe Interactions* 19(1): 33–42. DOI: 10.1094/MPMI-19-0033.

Collazo C, Giné-Bordonaba J, Aguiló-Aguayo I, Povedano I, Bademunt A and Viñas I (2018) *Pseudomonas graminis* strain CPA-7 differentially modulates the oxidative

509 response in fresh-cut ‘Golden delicious’ apple depending on the storage conditions.
510 *Postharvest Biology and Technology* 138(December 2017): 46–55. DOI:
511 10.1016/j.postharvbio.2017.12.013.

512 Crisosto CH and Valero D (2008) Harvesting and Postharvest Handling of Peaches for
513 the Fresh Market. In: Layne D and Bassi D (eds) *The Peach: Botany, Production*
514 *and Uses*. Wallingford, UK: CABI.

515 De Cal A, Sandín-España P, Martinez F, Egüen B, Chien-Ming C, Lee MH, Melgarejo
516 P and Prusky D (2013) Role of gluconic acid and pH modulation in virulence of
517 *Monilinia fructicola* on peach fruit. *Postharvest Biology and Technology* 86: 418–
518 423. DOI: 10.1016/j.postharvbio.2013.07.012.

519 Famiani F, Farinelli D, Moscatello S, Battistelli A, Leegood RC and Walker RP (2016)
520 The contribution of stored malate and citrate to the substrate requirements of
521 metabolism of ripening peach (*Prunus persica* L. Batsch) flesh is negligible.
522 Implications for the occurence of phosphoenolpyruvate carboxykinase and
523 gluconeogenesis. *Plant Physiology and Biochemistry* 101: 33–42. DOI:
524 10.1016/j.plaphy.2016.01.007.

525 Garcia-Benitez C, Melgarejo P and De Cal A (2017) Fruit maturity and post-harvest
526 environmental conditions influence the pre-penetration stages of Monilinia
527 infections in peaches. *International Journal of Food Microbiology* 241: 117–122.
528 DOI: 10.1016/j.ijfoodmicro.2016.09.010.

529 Génard M, Lescourret F, Gomez L and Habib R (2003) Changes in fruit sugar
530 concentrations in response to assimilate supply, metabolism and dilution: a
531 modeling approach applied to peach fruit (*Prunus persica*). *Tree Physiology*
532 23(March): 373–385. DOI: 10.1093/treephys/23.6.373.

533 Giné-Bordonaba J and Terry LA (2016) Effect of deficit irrigation and methyl
534 jasmonate application on the composition of strawberry (Fragaria x ananassa) fruit
535 and leaves. *Scientia Horticulturae* 199: 63–70. DOI:
536 10.1016/j.scienta.2015.12.026.

537 Giné-Bordonaba J, Echeverria G, Ubach D, Aguiló-Aguayo I, López ML and
538 Larrigaudière C (2017) Biochemical and physiological changes during fruit
539 development and ripening of two sweet cherry varieties with different levels of
540 cracking tolerance. *Plant Physiology and Biochemistry* 111: 216–225. DOI:
541 10.1016/j.plaphy.2016.12.002.

542 Guidarelli M, Zubini P, Nanni V, Bonghi C, Rasori A, Bertolini P and Baraldi E (2014)
543 Gene expression analysis of peach fruit at different growth stages and with
544 different susceptibility to *Monilinia laxa*. *European Journal of Plant Pathology*
545 140: 503–513. DOI: https://doi.org/10.1007/s10658-014-0484-8.

546 Hammond-Kosack KE and Jones JDG (1996) Resistance gene-dependent plant defense
547 responses. *The Plant Cell* 8(10): 1773–1791. DOI: 10.2307/3870229.

548 Kader AA and Saltveit ME (2003) Respiration and gas exchange. In: Bartz JA and
549 Brecht JK (eds) *Postharvest Phyisiology and Pathology of Vegetables*. 2nd ed.
550 New York: Marcel Dekker, Inc.

551 Kou J, Wei Y, He X, Xu J, Xu F and Shao X (2018) Infection of post-harvest peaches
552 by *Monilinia fructicola* accelerates sucrose decomposition and stimulates the
553 Embden-Meyerhof-Parnas pathway. *Horticulture Research* 5(46): 1–9. DOI:
554 https://doi.org/10.1038/s41438-018-0046-x.

555 Lattanzio VMTV, Lattanzio VMTV, Cardinali A, Amendola V and Imperato F (2006)
556 *Role of Phenolics in the Resistance Mechanisms of Plants against Fungal*

557 *Pathogens and Insects*. *Phytochemistry*. DOI: 10.1080/19439342.2018.1452778.

558 Lee M-H and Bostock RM. (2006) *Agrobacterium* T-DNA-mediated integration and
559 gene replacement in the brown rot pathogen *Monilinia fructicola*. *Current Genetics*
560 49(5): 309–322. DOI: 10.1007/s00294-006-0059-0.

561 Lee M-H and Bostock RM (2006) Induction, regulation and role in pathogenesis of
562 appressoria in *Monilinia fructicola*. *Phytopathology* 96: 1072–1080. DOI:
563 https://doi.org/10.1094/PHYTO-96-1072.

564 Lee M-H and Bostock RM (2007) Fruit exocarp phenols in relation to quiescence and
565 development of *Monilinia fructicola* infections in *Prunus* spp.: a role for cellular
566 redox? *Phytopathology* 97(3): 269–277. DOI: 10.1094/PHYTO-97-3-0269.

567 Lee M-H, Chiu C-M, Roubtsova T, Chou C-M and Bostock RM (2010) Overexpression
568 of a redox-regulated cutinase gene, *MfCUT1*, increases virulence of the brown rot
569 pathogen *Monilinia fructicola* on *Prunus* spp. *Molecular plant-microbe*
570 *interactions : MPMI* 23(2): 176–86. DOI: 10.1094/MPMI-23-2-0176.

571 Lindo-García V, Larrigaudière C, Echeverría G, Murayama H, Soria Y and Giné-
572 Bordonaba J (2019) New insights on the ripening pattern of 'Blanquilla' pears: A
573 comparison between on- and off-tree ripened fruit. *Postharvest Biology and*
574 *Technology* 150(January): 112–121. DOI: 10.1016/j.postharvbio.2018.12.013.

575 Meier U, Graf H, Hack H, et al. (1994) Phenological growth stages of pome fruits
576 (*Malus domestica* Borkh. and *Pyrus communis* L.), stone fruits (*Prunus* species),
577 currants (*Ribes* species) and strawberry (*Fragaria* × *ananassa* Duch.).
578 *Nachrichtenblatt des Deutschen Pflanzenschutzdienstes* 46: 141–153.

579 Mengiste T, Laluk K and AbuQamar S (2010) Mechanisms of induced resistance

against *B. cinerea*. In: Prusky D and Gullino ML (eds) *Post-Harvest Pathology, Plant Pathology in the 21st Century*. Springer.

Nonis A, Ruperti B, Falchi R, Casatta E, Thamasebi Enferadi S and Vizzotto G (2007) Differential expression and regulation of a neutral invertase encoding gene from peach (*Prunus persica*): evidence for a role in fruit development. *Physiologia Plantarum* 129(2): 436–446. DOI: 10.1111/j.1399-3054.2006.00832.x.

Oliveira Lino L, Génard M, Signoret V and Quilot-Turion B (2016) Physical host factors for brown rot resistance in peach fruit. *Acta Horticulturae* 1137: 105–112. DOI: 10.17660/ActaHortic.2016.1137.15.

Osorio S and Fernie AR (2013) Biochemistry of Fruit Ripening. In: Seymour GB, Poole M, Giovannoni JJ, and Tucker GA (eds) *The Molecular Biology and Biochemistry of Fruit Ripening*. Iowa, USA: John Wiley & Sons, Inc.

Pech JC, Bouzayen M and Latché A (2008) Climacteric fruit ripening: Ethylene-dependent and independent regulation of ripening pathways in melon fruit. *Plant Science* 175(1–2): 114–120. DOI: 10.1016/j.plantsci.2008.01.003.

Prusky D, Barad S, Ment D and Bi F (2016) The pH modulation by fungal secreted molecules: a mechanism affecting pathogenicity by postharvest pathogens. *Israel Journal of Plant Sciences* 63(1): 22–30. DOI: 10.1080/07929978.2016.1151290.

Prusky DB and Wilson RA (2018) Does increased nutritional carbon availability in fruit and foliar hosts contribute to modulation of pathogen colonization? *Postharvest Biology and Technology* 145: 27–32. DOI: 10.1016/j.postharvbio.2018.05.001.

Ramina A, Tonutti P and McGlasson W (2008) Ripening, Nutrition and Postharvest Physiology. In: Layne D and Bassi D (eds) *The Peach: Botany, Production and*

603 *Uses*. Wallingford, UK: CABI.

604 Rungjindamai N, Jeffries P and Xu XM (2014) Epidemiology and management of
605 brown rot on stone fruit caused by *Monilinia laxa*. *European Journal of Plant*
606 *Pathology* 140(1): 1–17. DOI: 10.1007/s10658-014-0452-3.

607 Shigenaga AM and Argueso CT (2016) No hormone to rule them all: Interactions of
608 plant hormones during the responses of plants to pathogens. *Seminars in Cell and*
609 *Developmental Biology* 56: 174–189. DOI: 10.1016/j.semcdb.2016.06.005.

610 Shokri H (2011) Evaluation of inhibitory effects of citric and tartaric acids and their
611 combination on the growth of *Trichophyton mentagrophytes*, *Aspergillus*
612 *fumigatus*, *Candida albicans*, and *Malassezia furfur*. *Comparative Clinical*
613 *Pathology* 20(5): 543–545. DOI: 10.1007/s00580-011-1195-6.

614 Tauzin AS and Giardina T (2014) Sucrose and invertases, a part of the plant defense
615 response to the biotic stresses. *Frontiers in Plant Science* 5(JUN): 1–8. DOI:
616 10.3389/fpls.2014.00293.

617 Villarino M, Sandín-España P, Melgarejo P and De Cal A (2011) High chlorogenic and
618 neochlorogenic acid levels in immature peaches reduce *Monilinia laxa* infection by
619 interfering with fungal melanin biosynthesis. *Journal of Agricultural and Food*
620 *Chemistry* 59(7): 3205–3213. DOI: 10.1021/jf104251z.

621 Wang GY, Michailides TJ, Hammock BD, Lee Y-M and Bostock RM (2002) Molecular
622 cloning, characterization, and expression of a redox-responsive cutinase from
623 *Monilinia fructicola* (Wint.) Honey. *Fungal genetics and biology* 35(3): 261–276.
624 DOI: 10.1006/fgbi.2001.1320.

625 Wang X, Ding Y, Wang Y, Pan L, Niu L, Lu Z, Cui G, Zeng W and Wang Z (2017)

626 Genes involved in ethylene signal transduction in peach (Prunus persica) and their
627 expression profiles during fruit maturation. *Scientia Horticulturae* 224(March):
628 306–316. DOI: 10.1016/j.scienta.2017.06.035.

629 Wold S (1995) PLS for Multivariate Linear Modeling. In: Waterbeemd H van (ed.)
630 *Chemometric Methods in Molecular Design*. Weinheim, Germany: VCH, p. 369.

631 Yang B, Yongcai L, Yonghong G and Yi W (2010) Mechanisms of induced resistance
632 against *B. cinerea*. In: Prusky D and Gullino ML (eds) *Post-Harvest Pathology,*
633 *Plant Pathology in the 21st Century*. Springer.

634

635

636

637

638

639

640

641

642

643

644

645

646

List of figures

Fig. 1. Changes in fruit weight (■) and diameter (●) of 'Merryl O'Henry' peach fruit during growth and ripening, expressed as d after full bloom (DAFB) (A). Each point represents the mean and vertical bars indicate the standard deviation of the mean (n = 4). Relationship between fruit weight and diameter calculated according to a polynomial linear regression (B). Image of the different phenological stages corresponding to each sampling point (C). In bold, phenological growth stages selected for the biochemical and susceptibility measurements (49, 77, 126 and 160 DAFB).

Fig. 2. Changes in ethylene production (pmol kg^{-1} s^{-1} C_2H_4; A or pmol s^{-1} C_2H_4 per fruit; B) and fruit respiration (nmol kg^{-1} s^{-1} CO_2; C or nmol s^{-1} CO_2 per fruit; D) of 'Merryl O'Henry' peach fruit at different phenological growth stages. The insert in Fig. 2C represents the calculated respiratory quotient (RQ). Each point represents the mean and vertical bars indicate the standard deviation of the mean (n = 4).

Fig. 3. Changes in soluble sugars (glucose (●), fructose (○) and sucrose (▼)) and organic acids (malic (●), citric (○) and gluconic (▼)) of 'Merryl O'Henry' peach fruit at different phenological growth stages. Data is expressed on a standard fresh weight basis (g kg^{-1}; A and C) and on fruit basis (g per fruit; B and D), respectively. Each point represents the mean and vertical bars indicate the standard deviation of the mean (n = 3). For each compound over time, mean values with the same letter are not significantly different according to analysis of variance (ANOVA) and Tukey's HSD test ($p < 0.05$).

Fig. 4. Changes in the fruit antioxidant capacity (AC) (○) (g kg^{-1} Fe^{3+}; A or g Fe^{3+} per fruit; B), total phenolic compounds (TPC) (●) (g kg^{-1} gallic acid equivalents (GAE); A or g GAE per fruit; B), ascorbic acid (AsA) (○) and dehydroascorbate (dhAsA) (●) (mg kg^{-1}; C or mg per fruit; D), and malondialdehyde (MDA) (●) (µmol kg^{-1}; E or µmol per fruit; F) of 'Merryl O'Henry' peach fruit at different phenological growth stages. Each point represents the mean and vertical bars indicate the standard deviation of the mean (n = 3). For each compound over time, mean values with the same letter are not significantly different according to analysis of variance (ANOVA) and Tukey's HSD test ($p < 0.05$).

Fig. 5. Changes in brown rot susceptibility of 'Merryl O'Henry' peach fruit inoculated with different strains of *Monilinia* spp. at 49, 77, 126 and 160 d after full bloom (DAFB). Fruit were inoculated by immersion for 60 s in a conidial suspension containing 10^5 conidia mL^{-1} of strain CPMC6 of *M. fructicola* (■) or strains CPML11 (■) and ML8L (□) of *M. laxa*, and incubated for 7 d at 20 °C and 100 % relative humidity. Each point represents the mean and vertical bars indicate the standard deviation of the mean (n = 4). Mean values with the same uppercase letter within the same strain or mean values with the same lowercase letter within the same phenological stage are not significantly different according to analysis of variance (ANOVA) and Tukey's HSD test ($p < 0.05$).

Fig. 6. Partial Least Squares (PLS) correlation loading plot depicting the contribution of each physiological and biochemical factors (green letters) to *Monilinia laxa* incidence (lnML8L; blue letters) of 'Merryl O'Henry' peach fruit at different phenological growth stages. Each cluster is coloured as follows: 49 DAFB (blue), 77 DAFB (yellow), 126 DAFB (green) and 160 DAFB (orange). The insert represent the variable importance plot

(VIP). Number of VIP > 0.8 (discontinuous red line) indicates that predictors are important in determining the two factors used in the PLS model.

Supplemental Fig. 1. Visualization of Spearman's rank correlation matrix between physiological and biochemical traits of 'Merril O'Henry' peach fruit. Circles above and below the diagonal report the correlation coefficients between traits expressed on a standard weight basis and on fruit basis, respectively. Colour intensity and the size of each circle are proportional to the correlation coefficients. White squares denote non-significant correlations ($p > 0.05$). Dry weight / fresh weight ratio (DW / FW); monosaccharides / disaccharides ratio (M / D) and respiratory quotient (RQ).

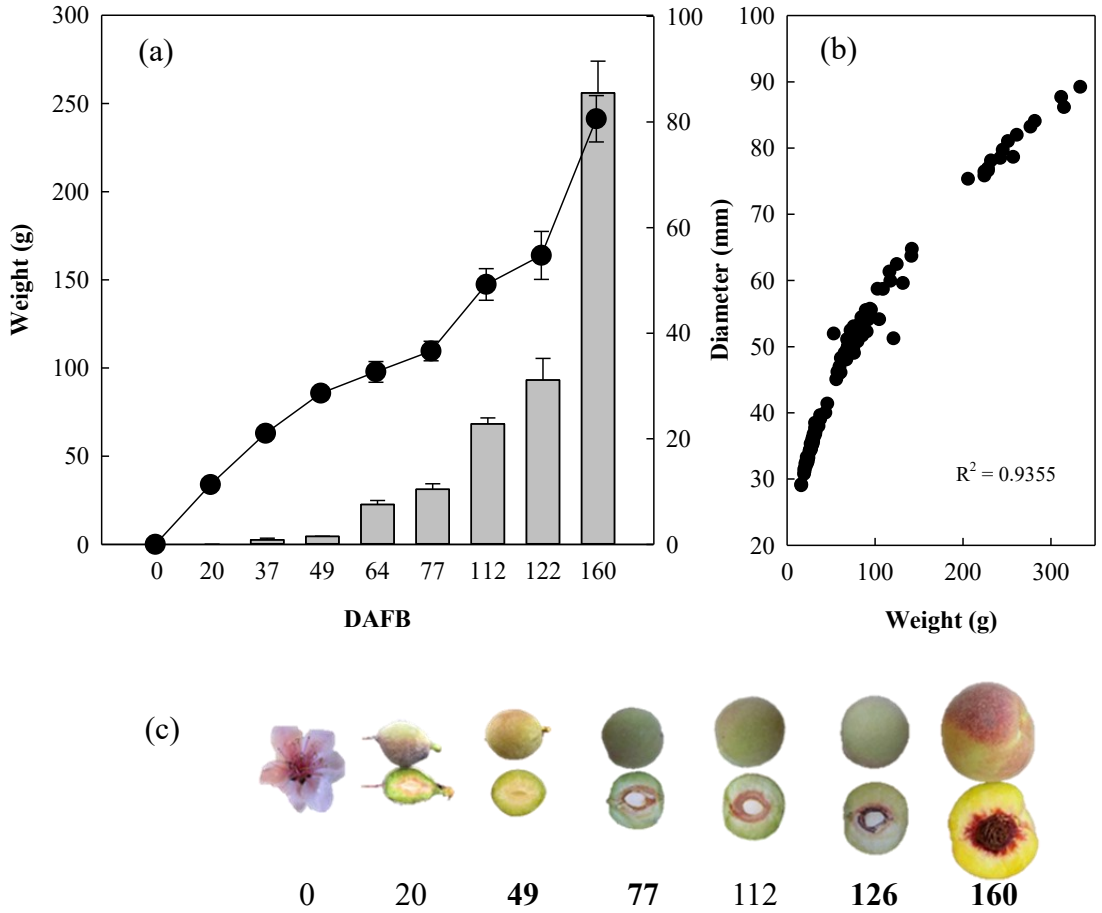
(a)
Weight (g)
DAFB
0 20 37 49 64 77 112 122 160
(b)
Diameter (mm)
Weight (g)
R² = 0.9355
(c)
0 20 49 77 112 126 160

Fig. 1.

741

742

743

744

745

746

747

748

749

750

751

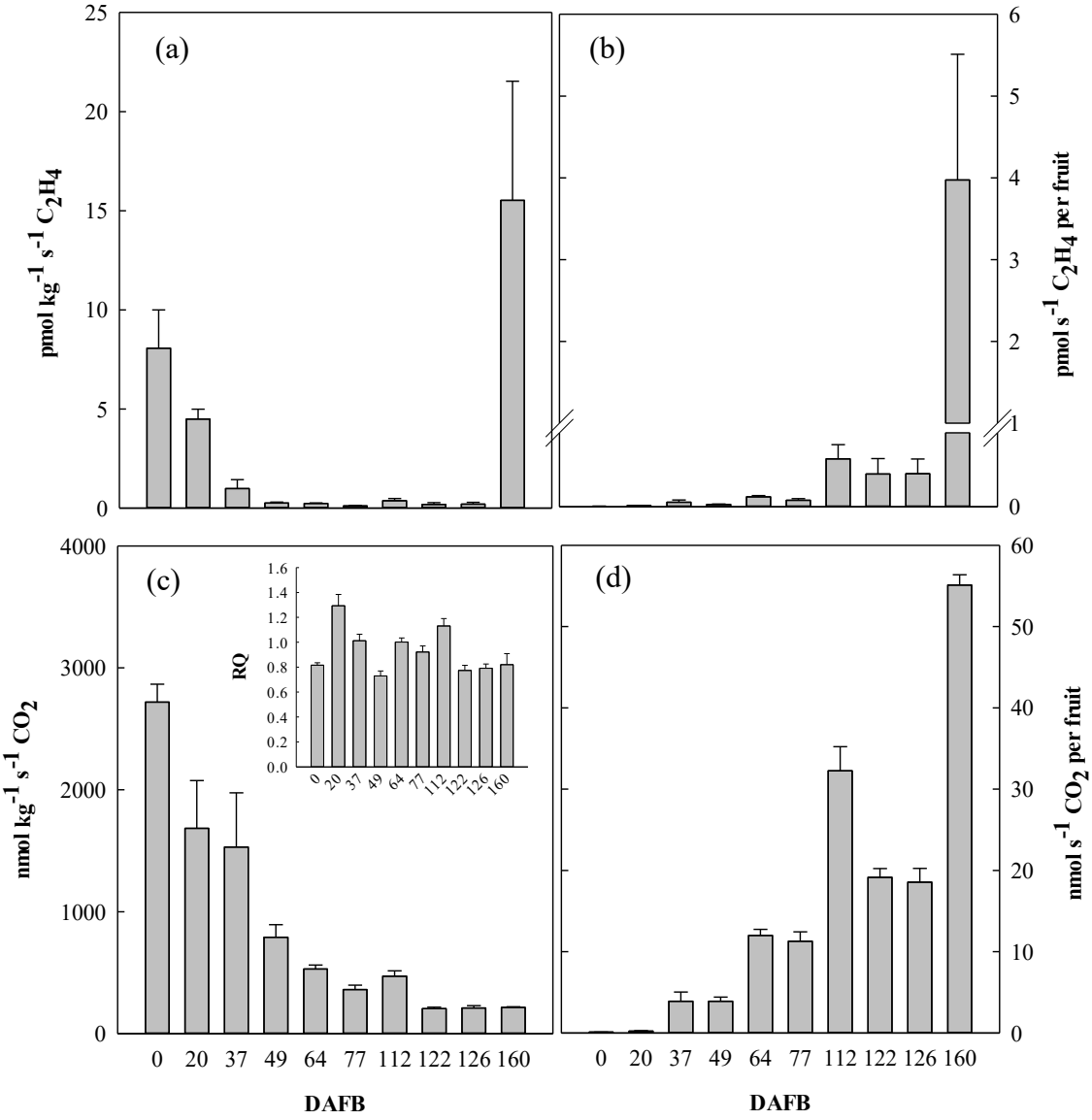

752

753

754 **Fig. 2.**

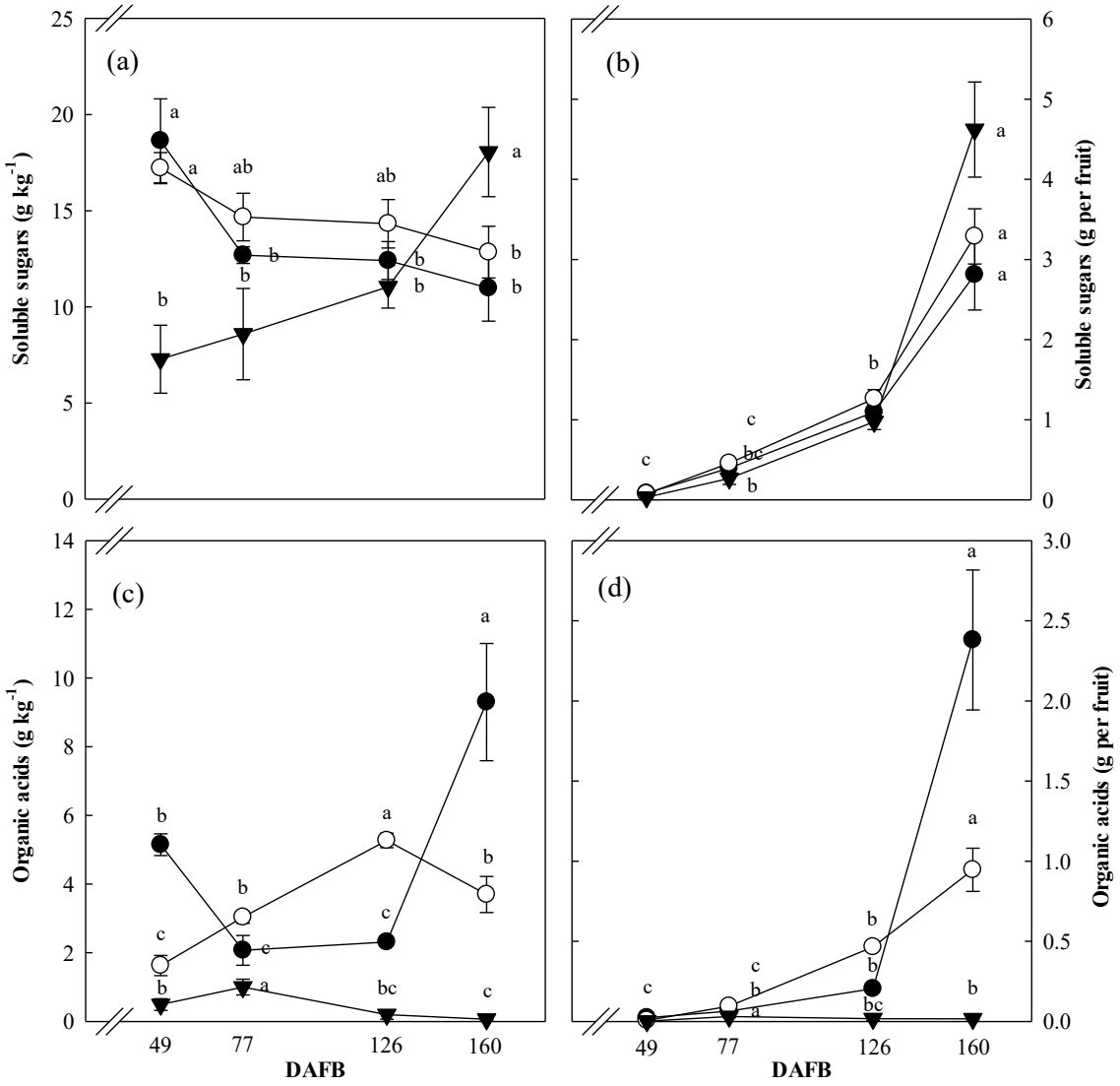
(a)
(b)
(c)
(d)
Soluble sugars (g kg-1)
Soluble sugars (g per fruit)
Organic acids (g kg-1)
Organic acids (g per fruit)
DAFB
DAFB
49
77
126
160

Fig. 3.

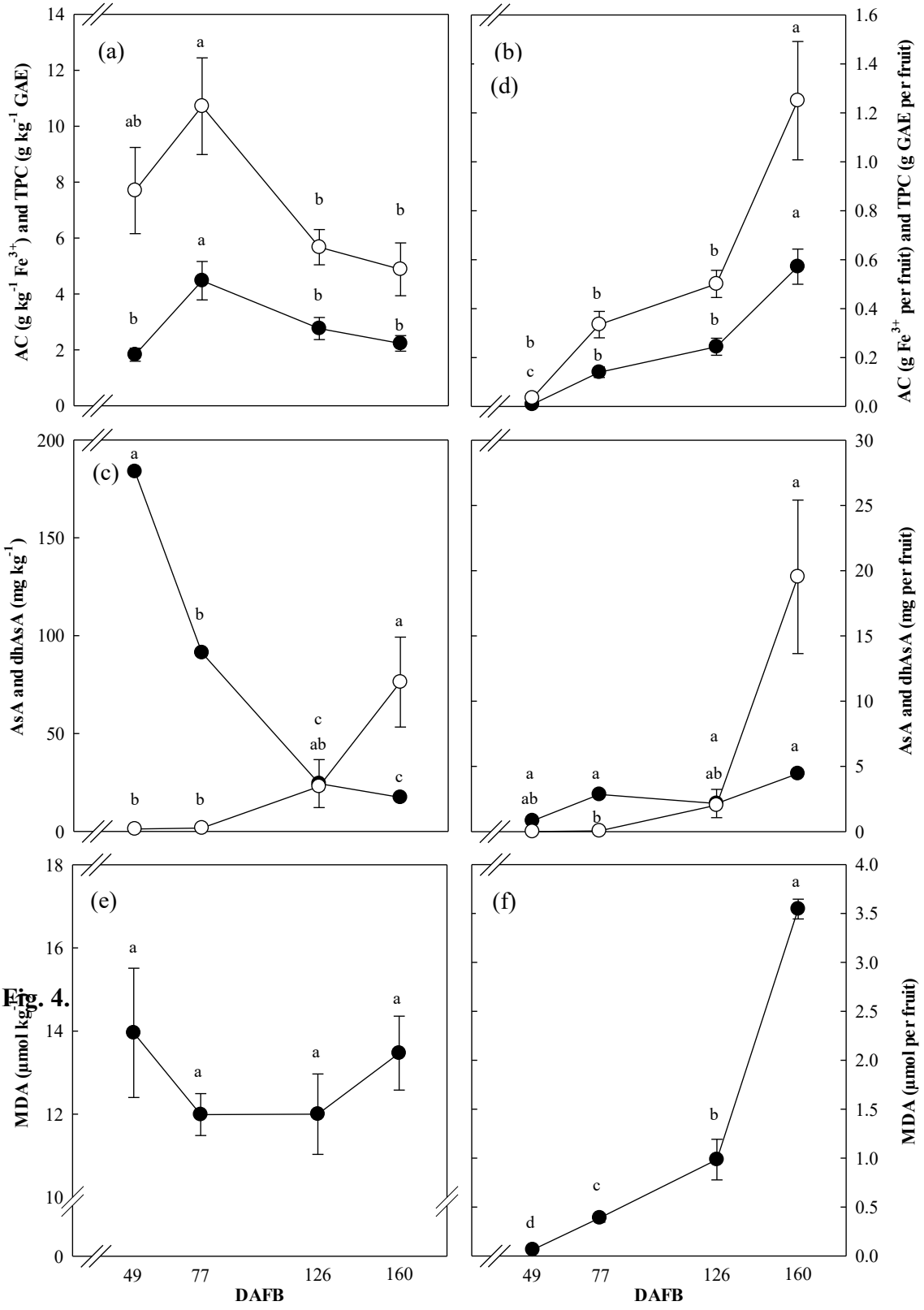
(a)
(b)
(d)
(c)
(e)
(f)
AC (g kg-1 Fe3+) and TPC (g kg-1 GAE)
AC (g Fe3+ per fruit) and TPC (g GAE per fruit)
AsA and dhAsA (mg kg-1)
AsA and dhAsA (mg per fruit)
MDA (µmol kg-1)
MDA (µmol per fruit)
DAFB
49
77
126
160

Fig. 4.

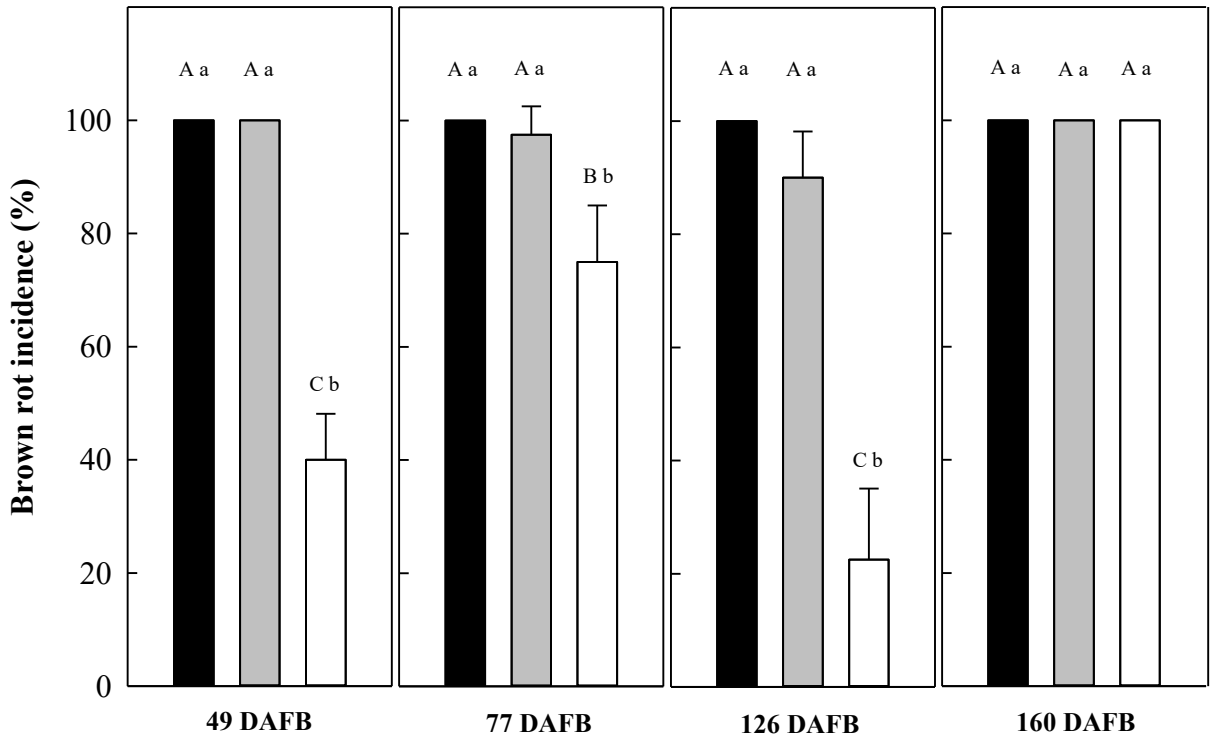
Brown rot incidence (%)
100
80
60
40
20
0
A a
A a
C b
A a
A a
B b
A a
A a
C b
A a
A a
A a
49 DAFB
77 DAFB
126 DAFB
160 DAFB

Fig. 5.

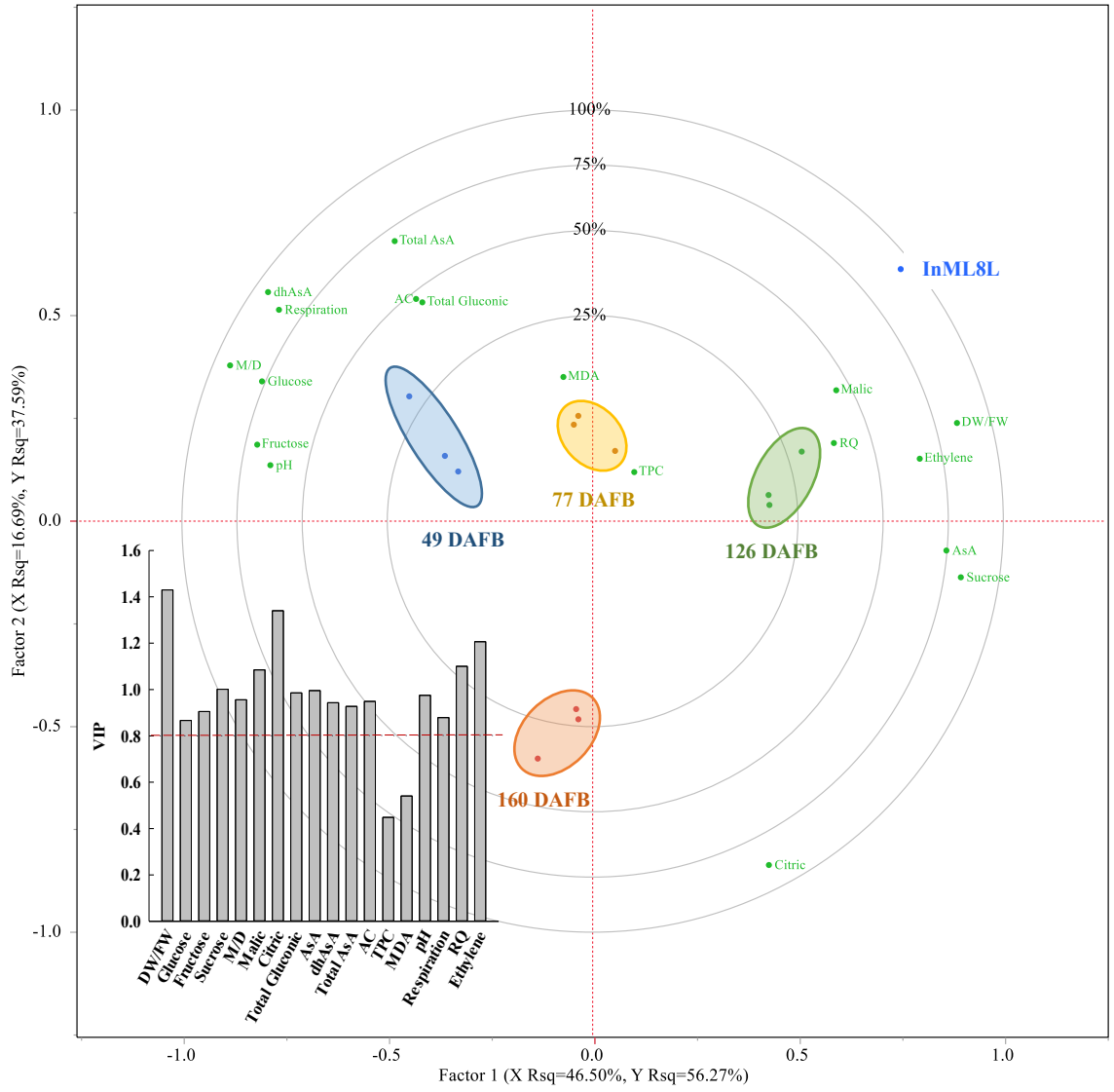
100%
75%
50%
25%
InML8L
Total AsA
dhAsA
Respiration
AC
Total Gluconic
M/D
Glucose
Fructose
pH
MDA
TPC
Malic
RQ
DW/FW
Ethylene
AsA
Sucrose
Citric
49 DAFB
77 DAFB
126 DAFB
160 DAFB
VIP
DW/FW
Glucose
Fructose
Sucrose
M/D
Malic
Citric
Total Gluconic
AsA
dhAsA
Total AsA
AC
TPC
MDA
pH
Respiration
RQ
Ethylene
Factor 1 (X Rsq=46.50%, Y Rsq=56.27%)
Factor 2 (X Rsq=16.69%, Y Rsq=37.59%)

Fig. 6.

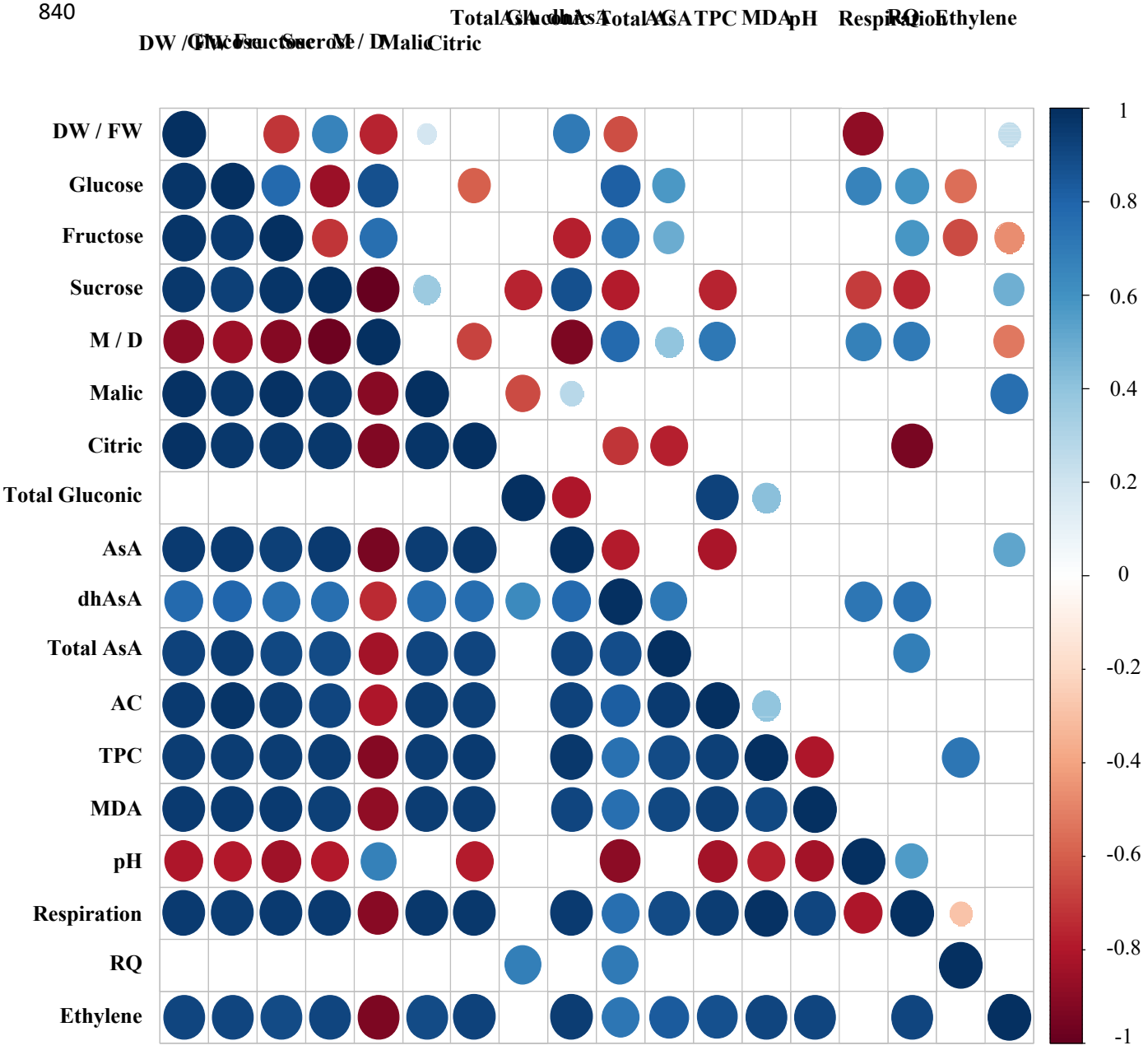

Supplemental Fig. 1. Visualization of Spearman's rank correlation matrix between physiological and biochemical traits of 'Merril O'Henry' peach fruit. Circles above and below the diagonal report the correlation coefficients between traits expressed on a standard weight basis and on fruit basis, respectively. Colour intensity and the size of each circle are proportional to the correlation coefficients. White squares denote non-significant correlations ($p > 0.05$). Dry weight / fresh weight ratio (DW / FW); monosaccharides / disaccharides ratio (M / D) and respiratory quotient (RQ).

884